



Underwater Acoustic Sensor Network Data Optimization with Enhanced Void Avoidance and Routing Protocol

¹ Meenakshi Garg, ² Sachin Sharma, ³ Mr. Vincent Balu, ⁴ Deepak K Sinha, ⁵ Dr. Pujita Bhatt, ⁶ Akash Kumar Bhagat,

¹ Assistant Professor, Department of Computer Science Engineering, Chandigarh Engineering College, Jhanjeri, India.
Orcid Id- 0000-0001-7112-7613

² Assistant Professor, Department of Computer Science and Engineering, Dev Bhoomi Uttarakhand University, Dehradun, Uttarakhand, India.

³ Head of Department, Department of Mechanical Engineering, Sanskriti University, Mathura, Uttar Pradesh, India.
Orcid Id- 0000-0002-7894-0444

⁴ Professor, Department of Computer Science and Engineering, Jain (Deemed-to-be University), Bangalore, India.
Orcid Id- 0000-0003-0317-8624

⁵ Assistant Professor, Department of Mechatronics, Parul Institute of Technology, Parul University, Vadodara, Gujarat, India.
Orcid Id- 0000-0002-9665-8186

⁶ Assistant Professor, Department of Computer Science, ARKA JAIN University, Jamshedpur, Jharkhand, India.
Orcid Id- 0000-0001-8717-764X

¹ meenakshi.j1888@cgc.ac.in, ² socse.sachin@dbuu.ac.in, ³ hodme@sanskriti.edu.in, ⁴ sk.deepak@jainuniversity.ac.in, ⁵ r.pujita.bhatt23607@paruluniversity.ac.in, ⁶ akash.b@arkajainuniversity.ac.in

Article History	Abstract
Received: 13 August 2022 Revised: 24 October 2022 Accepted: 12 November 2022	Deployment of a multi-hop underwater acoustic sensor network (UASN) in a larger region presents innovative challenges in reliable data communications and survivability of network because of the limited underwater interaction range or bandwidth and the limited energy of underwater sensor nodes. UASNs are becoming very significant in ocean exploration applications, like underwater device maintenance, ocean monitoring, ocean resource management, pollution detection, and so on. To overcome those difficulties and attains the purpose of maximizing data delivery ratio and minimizing energy consumption of underwater SNs, routing becomes necessary. In UASN, as the routing protocol will guarantee effective and reliable data communication from the source node to the destination, routing protocol model was an alluring topic for researchers. There were several routing techniques devised recently. This manuscript presents an underwater acoustic sensor network data optimization with enhanced void avoidance and routing (UASN-DAEVAR) protocol. The presented UASN-DAEVAR technique aims to present an effective data transmission process using proficient routing protocols. In the presented UASN-DAEVAR technique, a red deer algorithm (RDA) is employed in this study. In addition, the UASN-

<p>CC License CC-BY-NC-SA 4.</p>	<p>DAEVAR technique computes optimal routes in the UASN. To exhibit the effectual results of the UASN-DAEVAR technique, a wide spread experimental analysis is made. The experimental outcomes represented the enhancements of the UASN-DAEVAR model.</p> <p>Keywords: <i>Underwater acoustic sensor network; Routing protocol; Void avoidance; Metaheuristics; Red deer algorithm.</i></p>
---	--

1. Introduction

Practically 71% of our planet is covered by seas, and underwater networks become increasingly more significant since they can be utilized for underwater data trade, reconnaissance, sea investigations, and catastrophe avoidance, and so on, [1]. There are a few difficulties with underwater acoustic correspondence. To begin with, on the grounds that electromagnetic wave doesn't perform well in that frame of mind because of the serious constriction, acoustic correspondence is utilized as a significant correspondence innovation in underwater networks [2]. The acoustic channel is lopsided with enormous end-to-end spread postponements and restricted data transfer capacity as well as high piece blunder rates due to multi-path blurring. Second, underwater sensor hubs' versatility brought about by sea flows brings irregular connective connections [3]. Third, underwater sensor hubs are inclined to disappointment in view of consumption, fouling, and restricted battery power that is accessible. Moreover, the speed of the sound can change with water temperature, which prompts changes in the transmission way and might be the reason for the data not being sent to the ocean surface on time. In this way, the routing conventions accessible for earthly remote sensor networks are not appropriate for underwater acoustic sensor networks (UASNs), and many new routing conventions have been examined. Fig. 1 showcases the outline of UASN.

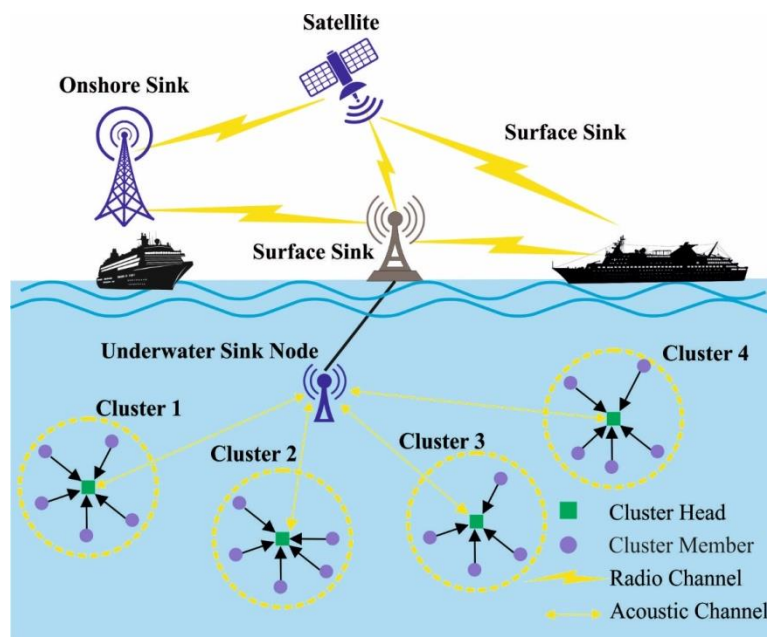


Fig. 1. Overview of UASN

There are a few studies on routing conventions for UASNs revealed in the writing, which give outlines about the fundamental thoughts of the connected conventions predominantly following the scientific categorization for earthly remote sensor networks [4]. In underwater acoustic correspondence because of changing the marine climate, connect quality varies quickly. It straightforwardly affects the presentation of networks like bundle conveyance proportion, delay, and so on. In a continuous situation, connect quality will differ with the distance between hub, profundity of the hub, and other underwater qualities like temperature, saltiness, delivering movement, pH

worth, and wind speed. The connection quality between hubs is dynamic and relies upon the underwater climate. However there are some underwater routing conventions, think about Packet Reception Ratio (PRR) as a proportion of connection quality, yet it won't definitively show the connection quality. The essential explanation is, aside from bundle drop because of diminished interface quality, the impact between parcels is additionally liable for dropping the bundle [5]. PRR is affecting the size of the parcel utilized. There is no component to separate between parcel drops because of the unfortunate connection quality and crash in remote media. Consequently, it is important to quantify the connection quality precisely and further involve that estimation in routing choice.

To effectively plan a data sending convention for UASNs, two issues should be painstakingly tended to since they exceptionally influence the presentation of the data sending conventions, to be specific, I) how to consider the portability of unreservedly drifting sensor hubs in unique underwater conditions to advance one data bundle through one single best way without the need to trade notice messages and ii) what are the forwarder determination rules to choose the best forwarder along the way among every one of the accessible ones [6]. To resolve the main issue, planning a data sending convention in light of a practical, genuinely motivated portability model that catches the elements of underwater hubs is critical. All in all, utilizing a reasonable versatility model assists with foreseeing the best way to the sink at the source hub level [7]. To deal with the subsequent issue, the data sending convention ought to pick the best way founded on the leftover energy of future adjoining hubs. To resolve the two issues, we propose a versatility expectation ideal data sending convention. As far as we could possibly know, an MPODF convention is the primary data sending convention that considers the practical versatility example of unreservedly drifting sensor hubs to foresee the best energy-productive way toward the sink and consequently stay away from warning messages' trade to lay out a way [8].

The central point that can influence the plan of a routing convention incorporates the quantity of sink hubs and the geography of the comparing UASN. Orchestrating numerous sink hubs in the network can further develop the routing execution by shortening transmission way. A sensor hub just has to communicate the parcels to the sink nearer to it [9]. Sending a UASN with static geography or a single-sink can improve the plan of a routing convention. A zero-sink-based UASN might have a few AUVs to fill in collectively, and it is harder to configure routing conventions for this sort of UASN to accomplish great execution. In the writing, many routing conventions are proposed, and a large portion of them depend on bounce count. However a hub can arrive at the sink with a base bounce count, it won't ensure that the parcel will arrive at the sink. One of the significant purposes behind bundle drop is the unfortunate connection nature of the way between the source and the sink [10]. The majority of the bounce based routing conventions expect that neighbors of the shipper/forwarder have profoundly dependable connections, and all have a similar connection quality. In this way, no significance is given to connect quality. It very well might be pertinent for earthly remote correspondence where connect quality continues as before or varies somewhat, yet it isn't relevant in underwater correspondence.

This manuscript presents an underwater acoustic sensor network data optimization with enhanced void avoidance and routing (UASN-DAEVAR) protocol. The presented UASN-DAEVAR technique aims to present an effective data transmission process using proficient routing protocols. In the presented UASN-DAEVAR technique, a red deer algorithm (RDA) is employed in this study. In addition, the UASN-DAEVAR technique computes optimal routes in the UASN. To exhibit the effectual results of the UASN-DAEVAR technique, a wide spread experimental analysis is made.

2. Existing Routing Protocols for UASN

The author in [11] developed reinforcement learning (RL) based opportunistic routing (OR) protocols (RLOR) by integrating the benefits of RL and OR algorithms. The presented technique is a type of distributed routing technique that expansively considers node exterior position to choose the proper relay node. Furthermore, a recovery system is applied in this work for enabling the packet to avoid the invalid region competently and continues to transmit which enhances the delivery rate of information in few sparse networks. In [12], a technique named an energy effective grid-based routing method (EEGBRP) for underwater WSN with TOPSIS approach and 3D cell partition is

presented. The projected technique is a multi-hop technique that in the primary phase is classified into 3D cells. Next, gateways or head-cell nodes are designated and information communication and routing can be implemented in the following stage.

In [13] proposed a Q-learning based energy effective and balanced data gathering (QL-EEBDG) routing method. In this work, the FN is chosen based on the RE and combined based on the neighboring node energy. Utilizing energy as the major selection variable guarantees effective energy utilization. Furthermore, effectual selection of FN rises the network lifespan. But the invalid node recovery procedure failed while the network topology is transformed. Singh and Gupta [14] introduced an energy effective optimum path routing for invalid evasion in UASN. The study applies the conception of GWO approach for calculating the fitness function and is utilized for selecting the better forwarder nodes in the network. The study considers the vertical direction that additionally decreases the end to end delay.

Chaaf et al. [15] developed relay-based void hole prevention and repair (ReVOHPR) protocols by autonomous underwater vehicles (AUV) for UWSNs. The presented study is a global solution that executes distinct stages of processes that equally act to resourcefully decrease and classify void holes and trap relay nodes for avoiding it. The study adopts the subsequent operation as ocean depth-based equivalent formation of the cluster, relay-assisted void hole repair, sleep schedules dynamically, and virtual graph-based routing. For energy effective cluster formation, entropy-based eligibility ranking (E2R) is developed that chooses stable CH. Next, dynamic sleep scheduling is executed using the dynamic kernel Kalman filter (DK2F) approach where the sleep and active modes are depending on the node's present condition. Anuradha et al. [16] developed a chaotic search-and-rescue-optimization-based multi-hop data transmission (CSRO-MHDT) technique for UWSN. While applying the presented method, CH is chosen and cluster is prearranged, which renders a range of features, involving intercluster detachment, RE, and intracluster distance. Furthermore, the presented technique is deliberated that is produced by integrating chaotic notions into the classical SRO technique.

3. The Proposed Model

This manuscript presented the UASN-DAEVAR technique to accomplish an effective data transmission process using proficient routing protocols. In the presented UASN-DAEVAR technique, the RDA is employed in this study. In addition, the UASN-DAEVAR technique computes optimal routes in the UASN.

The stages included to find a better result in RDA are discussed below [17]:

(1) Generation of RD

The size of N_{pop} arbitrary population is firstly produced for representing RD . The formula is given below:

$$RD = [R_1, R_2, R_3 \dots R_N] \tag{1}$$

In Eq. (1), R indicates a solution to the problem.

Then, the better RD from the population is gathered as male RD , N_{mak} where the residual population is described by the hinds (female RD s), N_{hind} . And it is evaluated in the following equation:

$$N_{hind} = N_{pop} - N_{male} \tag{2}$$

(2) Introduction of roaring amongst male RDs

Male RD has the possibility to improve their attractiveness by roaring in this phase. Compare the fitness values amongst its neighboring male RDs and each male RD and when the last one has better fitness value, its location is upgraded.

(

3) Selection of better male RD as male commander

Male RD shows dissimilar features with their capability to mate, roar, and attract hinds. Because of those variances, r percentage of the better males are only chosen as male commanders, N_{Com} , remaining male RDs are represented by, N_{stag} , as follow

$$N_{Com} = \text{round}\{r * N_{male}\} \quad (3)$$

$$N_{stag} = N_{male} - N_{Com} \quad (4)$$

(4) Introduction of fights between commanders and stags

Every commander randomly gets closer to each stag for individual fights. Then, two novel solutions (directions) are produced and the two primary ones which concern the stag and commander. The best fitness values replace the commander. In another word, the combat procedure allows better male RDs to be selected as commanders.

(5) Formation of harems

The amount of hinds allotted to the harem is proportionate to the commander's strength that is determined based on the decision criterion of commander. In observation, the best the fitness values of commander, the additional hinds are under the supervision as follows:

$$V_n = v_n - \max_i^{N_{Com}}\{v_j\} \quad (5)$$

Whereas v_n indicates the decision criterion of n^{th} commanders and V_n indicates the normalized values are represented in the following:

$$P_n = \left| \frac{V_n}{\sum_{i=1}^{N_{Com}} V_i} \right| \quad (6)$$

The amount of hinds for each harem controlled by every commander is evaluated by:

$$N.harern_n = \text{round}\{P_n * N_{hind}\} \quad (7)$$

In Eq. (7), $N.harern_n$ illustrates the amount of hinds, N_{hind} shows the n^{th} harems.

(6) Introduction of mating among female and male RDs

The mating procedure is significant in expanding the population of RDs. The stags and commanders mate with hind.

Commanders mate with α percentage of hinds in their harem

Every commander arbitrarily mates with α percentage of hind in the harem as follows

$$N.harern_n^{mate} = \text{round}\{\alpha * N.harern_n\} \quad (8)$$

In Eq. (11), $N.harern_n^{mate}$ indicates the amount of hinds chosen for mating in all the harems, n .

Commanders mate with β percentage of hinds in other harems

Next, all the commanders of harem mate with β percentage of hinds from arbitrarily selected harem k , excluding its own harem as follows

$$N.harern_k^{mate} = \text{round}\{\beta * N.harern_n\} \quad (9)$$

In Eq. (9), $N.harern_k^{mate}$ characterizes the amount of hinds in k^{th} harems.

The significance of these mating phases is the commander raises the territory size.

Mating of stags with the adjacent hinds

In conclusion, all the stags mate with hinds originate in its neighborhood. The distance between all the stags and i -th hinds is evaluated and the hind nearby to the stags is selected for the mating procedure.

$$d_j = \sqrt{j \in X_j(stag_j - hind_j^i)^2} \quad (10)$$

Whereas, the distance between all the stags and i -th hinds is represented by d_i . Fig. 2 represents the flowchart of RDO technique.

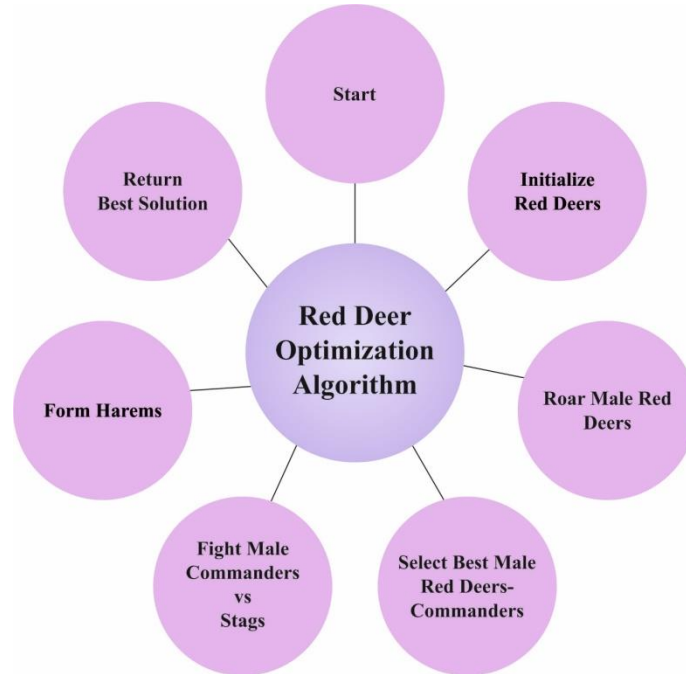


Fig. 2. Flowchart of RDO technique

(7) Selection of upcoming generation

The upcoming generation of RD is later chosen in two methods. Initially, a percent of better solution is chosen as a male RD that involves the stags and commanders. Next, the residual populations, viz., the hind are selected from the offspring and population of hinds previously produced by means of the roulette wheel selection algorithm.

For all the solutions, the fitness values are evaluated by mathematically modelling the distance shifted from one to other nodes.

The importance of FF has been related to CH being accessible from the technique, and supplementary places were combined in the sink. The reign of FF can be related to $m + 1$, where m defines the amount of CHs included in the network. Now, $F_i = (F_{i,1}(t), F_{i,2}(t) \dots F_{i,m+1}(t))$ indicate i^{th} FF, and the position $F_{i,d}, \forall i, 1 \leq i \leq m + 1, \forall d, 1 \leq d \leq m + 1$, designate next hop carried the dataset to BS. It was highly engrossed in unfolding optimal direction from CH to sink. It can be gained through FF in distinct sub-objectives for example, degree, distance, and node energy. To transfer data, next-hop achieves the data and sends them to BS. Following, supreme RE of next-hop was clearly ordered. Similarly, important sub-objective utilizing energy $f1$ was improvised by utilizing:

$$f1 = \sum_{i=1}^m E_{CHi} \quad (11)$$

As the distance between CH to sink and next-hop. Similarly, though the distance will be less compared to less the energy process rate was reduced. The detachment in Eq. (3) was employed for assessing the detachment among the two sensors [18]. Accept A and B as onward-moving devices and the detachment D between A and B can be assessed by the subsequent equation.

$$D_{ij} = \sqrt{(X_2 - X_1)^2 + (Y_2 - Y_1)^2} \quad (12)$$

In Eq. (12) the vertical and horizontal distances among sensors A and B indicate $(X_2 - X_1)$ and $(Y_2 - Y_1)$. The ' D_{ij} ' represents the detachment among two sensors.

$$D_{ij} = D(i, j), \text{edge}(i, j) \in R \quad (13)$$

Here ' D_{ij} ' indicates the detachment among sensors. R exemplifies a route among sensors. The ' i ' and ' j ' indicate limits in route R . Group of edges is called a route. As soon as sensor B becomes the beacon communication from sensor A , sensor B computes the precise distance among two sensors related to Eq. (12) [19].

The subsequent drive to reduce the distance between CHs to sink can be measured via:

$$f2 = \frac{1}{\sum_{i=1}^m \text{dis}(\text{CH}_i, \text{NH}) + \text{dis}(\text{NH}, \text{BS})} \quad (14)$$

Finally, node degree is designated related to the node degree of $f3$:

$$f3 = \frac{1}{\sum_{i=1}^m 1_i} \quad (15)$$

Formerly, the weighted sum can be executed for sub objectives and changed to separate objectives. Now, α_1, α_2 & α_3 signifies the weight selected to every subobjectives, and $\alpha_i \in (0, 1)$ and $\alpha_1 + \alpha_2 + \alpha_3 = 1$.

$$\text{Fitness} = \alpha_1(f1) + \alpha_2(f2) + \alpha_3(f3) \quad (16)$$

4. Performance Evaluation

The experimental validation of the UASN-DAEVAR model is carried out in this section. Table 1 and Fig. 3 provide a detailed energy tax (ENT) examination of the UASN-DAEVAR model with other models. The results indicated that the UASN-DAEVAR model has reached reduced ENT values under all NR. For instance, NR=100m, the UASN-DAEVAR model has attained decreased ENT of 0.00000010J. In addition, NR=200m, the UASN-DAEVAR method has obtained reduced ENT of 0.00000016J. Along with that, NR=400m, the UASN-DAEVAR technique has accomplished reduced ENT of 0.00000032J. Moreover, NR=600m, the UASN-DAEVAR approach has obtained reduced ENT of 0.00000048J.

Table 1 ENT analysis of UASN-DAEVAR approach with existing algorithms

Energy Tax (J)				
Network Radius (m)	EBDG	QL-EBDG	QL-EBDG-AND	UASN-DAEVAR
100	0.00000010	0.00000010	0.00000016	0.00000010
200	0.00000029	0.00000029	0.00000045	0.00000016
300	0.00000097	0.00000074	0.00000110	0.00000016
400	0.00000136	0.00000110	0.00000256	0.00000032
500	0.00000224	0.00000220	0.00000350	0.00000032
600	0.00000327	0.00000288	0.00000590	0.00000048
700	0.00000626	0.00000554	0.00000603	0.00000055
800	0.00000791	0.00000635	0.00000736	0.00000055
900	0.00001099	0.00000882	0.00000820	0.00000074
1000	0.00000914	0.00000554	0.00000781	0.00000068

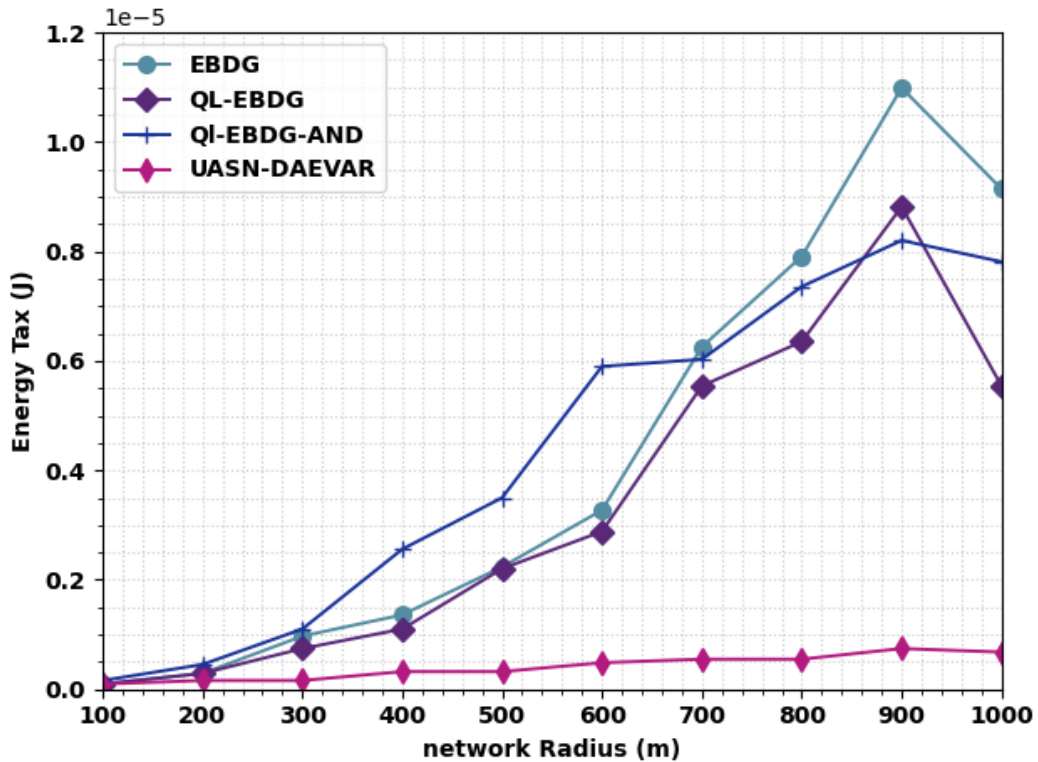


Fig. 3. ENT analysis of UASN-DAEVAR approach with existing algorithms

Table 2 and Fig. 4 indicate a detailed comparative NLT inspection of the UASN-DAEVAR model. The results implied that the UASN-DAEVAR model has shown enhanced NLT values under all NR. For instance, on NR of 100m, the UASN-DAEVAR model has offered increased NLT of 9964 rounds whereas the EBDG, QL-EBDG, and QL-EBDG-AND models have attained reduced NLT of 9983, 9964, and 9946 rounds correspondingly. Moreover, on NR of 500m, the UASN-DAEVAR method has provided improved NLT of 9964 rounds while the EBDG, QL-EBDG, and QL-EBDG-AND approaches have accomplished NLT of 9358, 9450, and 9046 rounds correspondingly. Furthermore, on NR of 1000m, the UASN-DAEVAR method has offered improved NLT of 8954 rounds while the EBDG, QL-EBDG, and QL-EBDG-AND methods have accomplished reduced NLT of 3258, 3846, and 3240 rounds correspondingly.

Table 2 NLT analysis of UASN-DAEVAR approach with existing algorithms under distinct NR

Network Lifetime (Rounds)				
Network Radius (m)	EBDG	QL-EBDG	QL-EBDG-AND	UASN-DAEVAR
100	9983	9964	9946	9964
200	9983	9928	9946	9983
300	9946	9956	9983	9982
400	9891	9928	9817	9981
500	9358	9450	9046	9964
600	8421	8403	8109	9891
700	7282	7300	6767	9909
800	6069	6124	5426	9670
900	4287	4507	3919	9431
1000	3258	3846	3240	8954

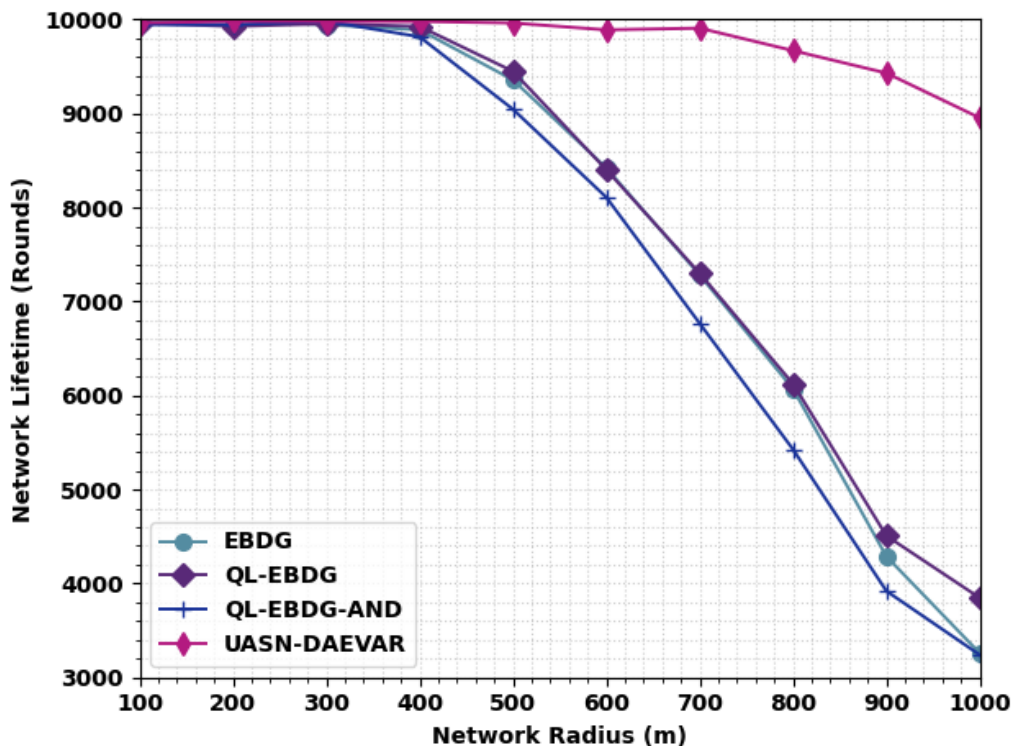


Fig. 4. NLT analysis of UASN-DAEVAR approach under distinct NR

Table 3 and Fig. 5 specify a detailed comparative network stability period (NSP) inspection of the UASN-DAEVAR model. The results demonstrate that the UASN-DAEVAR method has demonstrated improved NSP values under all NR. For example, on NR of 200m, the UASN-DAEVAR technique has improved NSP of 4621 while the EBDG, QL-EBDG, and QL-EBDG-AND methods have attained reduced NSP of 86, 205, and 165 correspondingly. Furthermore, on NR of 500m, the UASN-DAEVAR method has provided improved NSP of 11344 while the EBDG, QL-EBDG, and QL-EBDG-AND approaches have accomplished decreased NSP of 4820, 8201, and 10151 correspondingly. Additionally, on NR of 1000m, the UASN-DAEVAR method has provided improved NSP of 14646 while the EBDG, QL-EBDG, and QL-EBDG-AND approaches have accomplished decreased NSP of 3149, 5377, and 4541 correspondingly.

Table 3 NSP analysis of UASN-DAEVAR approach with existing algorithms under distinct NR

Network Stability Period				
Network Radius (m)	EBDG	QL-EBDG	QL-EBDG-AND	UASN-DAEVAR
100	0	0	0	0
200	86	205	165	4621
300	2433	2990	6053	7843
400	4223	6053	8162	9753
500	4820	8201	10151	11344
600	5456	9872	11185	11981
700	5894	10588	9594	12776
800	4502	8957	7644	13691
900	3308	5934	5934	14447
1000	3149	5377	4541	14646

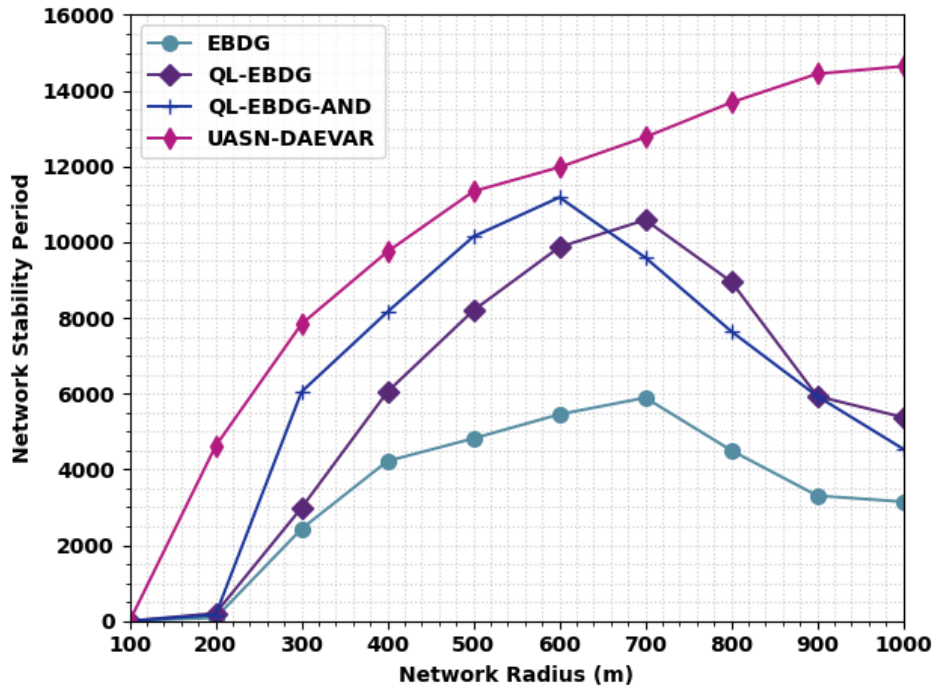


Fig. 5. NSP analysis of UASN-DAEVAR approach under distinct NR

Table 4 and Fig. 6 denotes a detailed comparative number of packet received (NOPR) examination of the UASN-DAEVAR technique. The outcomes show that the UASN-DAEVAR approach has demonstrated improved NOPR values under all NR. For example, on NR of 100m, the UASN-DAEVAR technique has provided improved NOPR of 489091 while the EBDG, QL-EBDG, and QL-EBDG-AND approaches have accomplished decreased NOPR of 325232, 380259, and 476862 correspondingly.

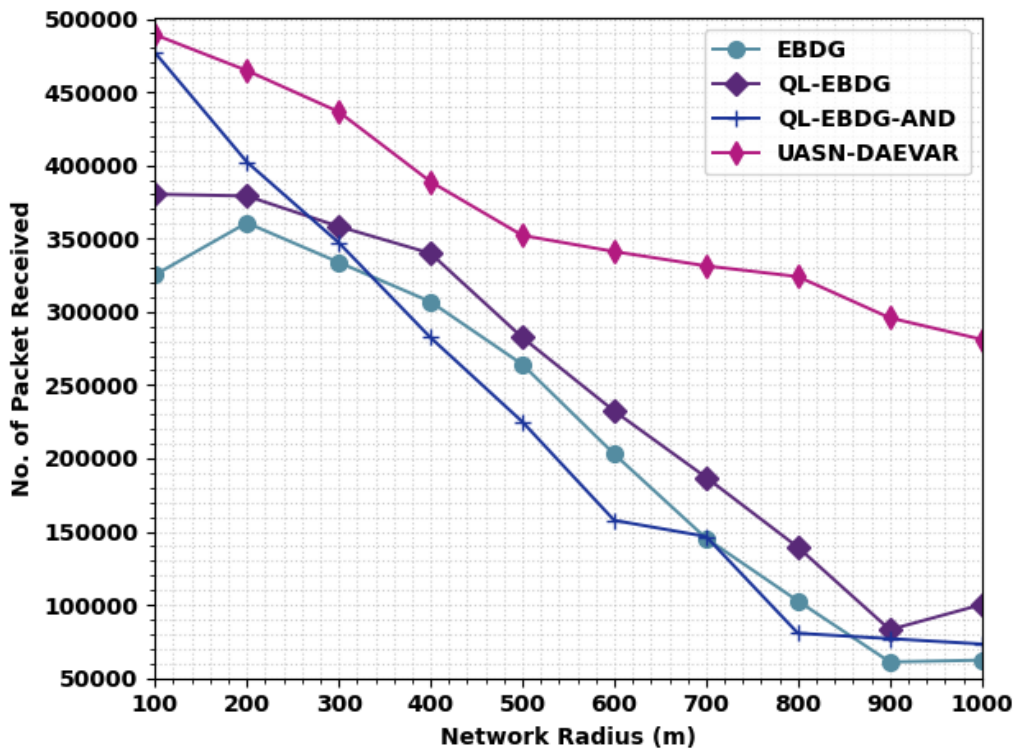


Fig. 6. NOPR analysis of UASN-DAEVAR approach under distinct NR

Table 4 NOPR analysis of UASN-DAEVAR approach with existing algorithms under distinct NR

No. of Packet Received				
Network Radius (m)	EBDG	QL-EBDG	QL-EBDG-AND	UASN-DAEVAR
100	325232	380259	476862	489091
200	360694	379037	402270	464634
300	333792	358249	347243	436509
400	306890	339906	282434	388819
500	264091	282434	224961	352135
600	202950	232298	157706	341129
700	145478	187054	146701	331347
800	102679	139364	80668	324010
900	61103	83114	77000	295885
1000	62326	100233	73331	281211

Furthermore, on NR of 500m, the UASN-DAEVAR approach has given improved NOPR of 352135 while the EBDG, QL-EBDG, and QL-EBDG-AND approach have accomplished reduced NOPR of 264091, 282434, and 224961 correspondingly. Furthermore, on NR of 1000m, the UASN-DAEVAR system has provided improved NOPR of 281211 whereas the EBDG, QL-EBDG, and QL-EBDG-AND models have attained reduced NOPR of 62326, 100233, and 73331 correspondingly.

Table 5 PDR analysis of UASN-DAEVAR approach with existing algorithms under distinct NR

Packet Delivery Ratio (%)				
Network Radius (m)	EBDG	QL-EBDG	QL-EBDG-AND	UASN-DAEVAR
100	98.13	98.13	98.13	98.69
200	97.66	98.03	97.75	98.41
300	96.15	97.19	97.09	98.79
400	93.51	95.87	97.00	98.22
500	90.97	89.37	93.14	97.75
600	87.96	85.51	90.69	96.34
700	82.97	84.10	88.34	94.83
800	76.66	81.94	85.79	92.57
900	72.80	78.26	81.94	88.53
1000	71.01	75.91	77.42	85.61

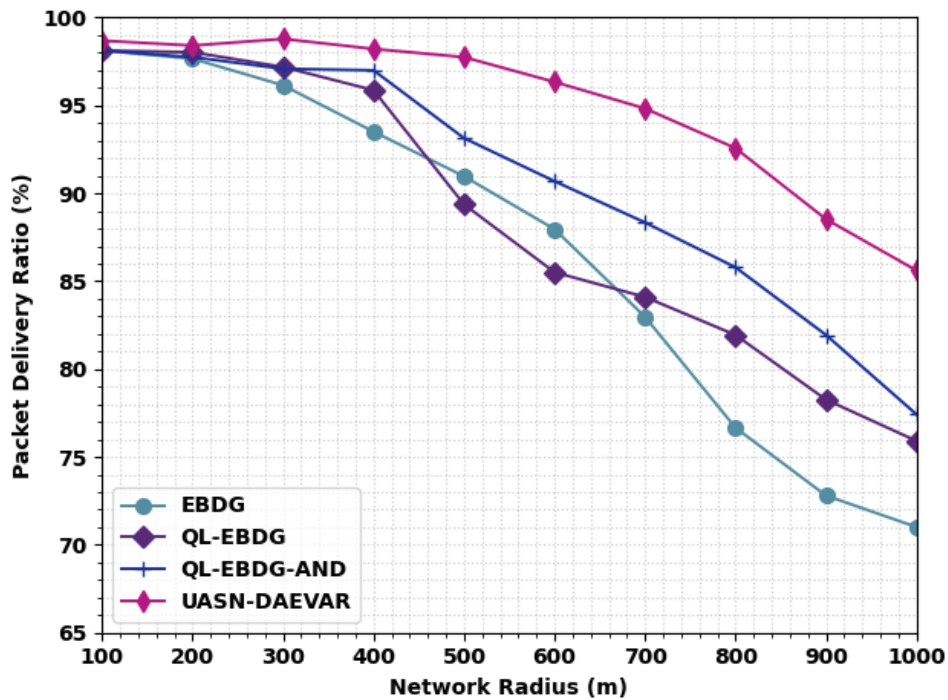


Fig. 7. PDR analysis of UASN-DAEVAR approach under distinct NR

Table 5 and Fig. 7 illustrate a detailed comparative PDR inspection of the UASN-DAEVAR technique. The outcomes show that the UASN-DAEVAR approach has demonstrated improved PDR values under all NR. For example, on NR of 100m, the UASN-DAEVAR method has offered increased PDR of 98.69% while the EBDG, QL-EBDG, and QL-EBDG-AND models have accomplished decreased PDR of 98.13%, 98.13%, and 98.13% correspondingly. Furthermore, on NR of 500m, the UASN-DAEVAR method has provided improved PDR of 97.75% while the EBDG, QL-EBDG, and QL-EBDG-AND models have attained reduced PDR of 90.97%, 89.37%, and 93.14% correspondingly. Additionally, on NR of 1000m, the UASN-DAEVAR model has provided improved PDR of 85.61% while the EBDG, QL-EBDG, and QL-EBDG-AND methods have accomplished decreased PDR of 71.01%, 75.91%, and 77.42% correspondingly.

5. Conclusion

This manuscript presented the UASN-DAEVAR technique to accomplish an effective data transmission process using proficient routing protocols. In the presented UASN-DAEVAR technique, the RDA is employed in this study. In addition, the UASN-DAEVAR technique computes optimal routes in the UASN using the behaviour of red deer's. To exhibit the effectual results of the UASN-DAEVAR technique, a wide spread experimental analysis is made. The experimental outcomes represented the enhancements of the UASN-DAEVAR model. Thus, the UASN-DAEVAR technique can be utilized to achieve effectual communication in real time platform.

References

- [1] Faheem, M., Butt, R.A., Raza, B., Alquhayz, H., Ashraf, M.W., Raza, S. and Ngadi, M.A.B., 2020. FFRP: dynamic firefly mating optimization inspired energy efficient routing protocol for internet of underwater wireless sensor networks. *IEEE Access*, 8, pp.39587-39604.
- [2] Khasawneh, A.M., Abualigah, L. and Al Shinwan, M., 2020, May. Void aware routing protocols in underwater wireless sensor networks: variants and challenges. In *Journal of physics: conference series* (Vol. 1550, No. 3, p. 032145). IOP Publishing.
- [3] Sher, A., Khan, A., Javaid, N., Ahmed, S.H., Aalsalem, M.Y. and Khan, W.Z., 2018. Void hole avoidance for reliable data delivery in IoT enabled underwater wireless sensor networks. *Sensors*, 18(10), p.3271.

- [4] Hussain, T., Rehman, Z.U., Iqbal, A., Saeed, K. and Ali, I., 2020. Two hop verification for avoiding void hole in underwater wireless sensor network using SM-AHH-VBF and AVH-AHH-VBF routing protocols. *Transactions on Emerging Telecommunications Technologies*, 31(8), p.e3992.
- [5] Kumari, S., Mishra, P.K. and Anand, V., 2020. Integrated load balancing and void healing routing with Cuckoo search optimization scheme for underwater wireless sensor networks. *Wireless Personal Communications*, 111(3), pp.1787-1803.
- [6] Haque, K.F., Kabir, K.H. and Abdelgawad, A., 2020. Advancement of routing protocols and applications of underwater wireless sensor network (UWSN)—A survey. *Journal of Sensor and Actuator Networks*, 9(2), p.19.
- [7] Teekaraman, Y., Sthapit, P., Choe, M. and Kim, K., 2019. Energy analysis on localization free routing protocols in UWSNs. *International Journal of Computational Intelligence Systems*, 12(2), pp.1526-1536.
- [8] Xiao, X. and Huang, H., 2020. A clustering routing algorithm based on improved ant colony optimization algorithms for underwater wireless sensor networks. *Algorithms*, 13(10), p.250.
- [9] Islam, T. and Lee, Y.K., 2019. A comprehensive survey of recent routing protocols for underwater acoustic sensor networks. *Sensors*, 19(19), p.4256.
- [10] Wan, Z., Liu, S., Ni, W. and Xu, Z., 2019. An energy-efficient multi-level adaptive clustering routing algorithm for underwater wireless sensor networks. *Cluster Computing*, 22(6), pp.14651-14660.
- [11] Zhang, Y., Zhang, Z., Chen, L. and Wang, X., 2021. Reinforcement learning-based opportunistic routing protocol for underwater acoustic sensor networks. *IEEE Transactions on Vehicular Technology*, 70(3), pp.2756-2770.
- [12] Noorbakhsh, H. and Soltanaghaei, M., 2022. EEGBRP: an energy-efficient grid-based routing protocol for underwater wireless sensor networks. *Wireless Networks*, pp.1-15.
- [13] Khan, Z.A., Karim, O.A., Abbas, S., Javaid, N., Zikria, Y.B. and Tariq, U., 2021. Q-learning based energy-efficient and void avoidance routing protocol for underwater acoustic sensor networks. *Computer Networks*, 197, p.108309.
- [14] Singh, B. and Gupta, B., 2022. An Energy Efficient Optimal Path Routing (EEOPR) for Void Avoidance in Underwater Acoustic Sensor Networks. *International Journal of Computer Network & Information Security*, 14(3).
- [15] Chaaf, A., Saleh Ali Muthanna, M., Muthanna, A., Alhelaly, S., Elgendy, I.A., Iliyasu, A.M., El-Latif, A. and Ahmed, A., 2021. Energy-efficient relay-based void hole prevention and repair in clustered multi-AUV underwater wireless sensor network. *Security and Communication Networks*, 2021.
- [16] Anuradha, D., Subramani, N., Khalaf, O.I., Alotaibi, Y., Alghamdi, S. and Rajagopal, M., 2022. Chaotic search-and-rescue-optimization-based multi-hop data transmission protocol for underwater wireless sensor networks. *Sensors*, 22(8), p.2867.
- [17] Fazli, M., Fathollahi-Fard, A.M. and Tian, G., 2019. Addressing a coordinated quay crane scheduling and assignment problem by red deer algorithm. *International Journal of Engineering*, 32(8), pp.1186-1191.
- [18] Moridi, E. and Barati, H., 2017. RMRPTS: a reliable multi-level routing protocol with tabu search in VANET. *Telecommunication Systems*, 65(1), pp.127-137.
- [19] Ramamoorthy, R. and Thangavelu, M., 2022. An enhanced hybrid ant colony optimization routing protocol for vehicular ad-hoc networks. *Journal of Ambient Intelligence and Humanized Computing*, 13(8), pp.3837-3868.